Theoretical and experimental investigations of the electronic structure for selectively δ-doped strained $In_xGa_{1-x}As/GaAs$ quantum wells

Mao-long Ke, D. Westwood, and R. H. Williams
Department of Physics and Astronomy, University of Wales College of Cordiff, Cardiff CF2 3YB, United Kingdom

M. J. Godfrey
Department of Pure and Applied Physics, University of Manchester Institute of Science and Technology, Manchester M60 1QD, United Kingdom

(Received 12 August 1994)

The electronic structures of Si δ-doped strained $In_xGa_{1-x}As/GaAs$ quantum wells have been studied theoretically and compared with experiments. The emphasis has been on the comparison between well center-, edge-, and barrier-positioned δ-doped layers. The highest achievable single-subband occupation decreases as the δ sheet is moved away from the center to the edge and finally to the barrier, but the electron mobility increases at the same time. Photoluminescence data have been found shifted to lower energies than the predictions of a self-consistent Hartree calculation owing to many-body effects, which have been quantified here using both plasmon-pole and random-phase approximations.

I. INTRODUCTION

The δ-doping technique has been used widely to introduce carrier-confinement effects[1-4] and potential-barrier modulation.[5,6] Recently, there has been a growing interest in combining the δ-doping technique with compositional quantum wells in order to achieve an extra degree of band-structure engineering. However, most of the work so far has concentrated on the center δ-doped GaAs-$Al_xGa_{1-x}As$ systems.[7-11] Although this system has the advantage of achieving high densities of two-dimensional electron gas (2DEG),[7,8] it gives only very limited electron mobility. Logically, this mobility limit can be surpassed by the δ-modulation-doping technique, in which a δ sheet is placed inside the barrier rather than inside the well. Systems of this kind may provide a method of achieving both a high density of 2DEG and high electron mobility.[12,13] We study them in detail here. Further, Masselink[8] has very recently reported that an off-center δ-doped (midway between center and edge) quantum well has a higher electron mobility than the center δ-doped quantum well. Here we shall look at the luminescence property and the electron mobility for both the center and the edge δ-doped structure. We are especially interested in the comparative behavior among the various δ-doped systems.

The host material used in the present paper is the $In_xGa_{1-x}As$-GaAs strained system. Its advantage over the commonly used $GaAs/Al_xGa_{1-x}As$ is that the $Al_xGa_{1-x}As$ barrier suffers from the presence of *DX* centers in the case of heavy doping. Also, the control of impurity spread is more difficult to achieve in $Al_xGa_{1-x}As$ than GaAs owing to the higher growth temperature required.

The paper is organized as follows: in Sec. II we present the results of self-consistent calculations of the electronic structure for some δ-doped strained quantum-well systems. A comparison will be made between the various δ-positioned structures (center, interface, or barrier). In Sec. III we examine some experimental data in the light of our calculated results. Band-gap renormalizations due to many body effects are discussed in Sec. IV. Finally, our conclusions appear in Sec. V.

II. SELF-CONSISTENT CALCULATIONS

Our structures consist of a thick GaAs buffer grown on a GaAs substrate, followed by a thin $In_xGa_{1-x}As$ active layer and terminated with a 500-Å GaAs capping layer. Accordingly, the GaAs layer can be assumed to be unstrained, so that lattice mismatch between $In_xGa_{1-x}As$ and GaAs layers is accommodated by compressional strain of the $In_xGa_{1-x}As$. The main result of the $In_xGa_{1-x}As$ compression is an increase in the band gap and separation of the heavy- and light-hole valence bands.[14-16] Some modification of the conduction band also occurs. Such strain-induced effects on the $In_xGa_{1-x}As$ band structure can be estimated from multiband $\mathbf{k}\cdot\mathbf{p}$ calculations,[15-17] but uncertainties in the valence-band parameters are still a significant source of error in any effective-mass calculation. The band offset is also required for the subband-structure calculation, and much uncertainty exists so far in the literature of the $GaAs/In_xGa_{1-x}As$ system. Fortunately, it does not alter the subband-energy level appreciably. Another uncertainty is the accuracy of the In composition. Experimentally, the In concentration cannot be controlled to a desirable precision, and accurate knowledge of the In concentration is important here for the detailed comparison between theory and experiment. At present we believe that the best way forward is to make comparison against a reference undoped sample grown under identical conditions.

We have calculated the electronic structure for the Si

δ-doped $In_xGa_{1-x}As$-GaAs quantum wells by solving the Poisson and Schrödinger equations self-consistently. The effects of nonparabolicity and Fermi-level pinning are included in the calculation. Because the Fermi level at the quantum-well region is not known *a priori*, the amount of charge transferred into surface states due to the pinning must be determined self-consistently. When exchange and correlation effects are incorporated using the local-density-functional formalism we find little change to the energy levels of carriers. Certainly we cannot explain in this way the experimentally observed narrowing of the band gap.

Numerical results

In our calculation we have taken the strained $In_xGa_{1-x}As$ gap E_g and the effective mass from Ref. 15, and conduction-band offset $V_c=0.7\Delta E_g$. The GaAs background is assumed to be p type at a level of 5×10^{14} cm^{-3}, which represents the worst case for our molecular-beam-epitaxy (MBE) grown layer. The conduction-band potential profiles and the corresponding electronic distributions for center, interface, and barrier δ-doped structures are shown in Fig. 1. The parameters used are In composition $x=0.265$, doping density $N_D=2\times10^{12}$ cm^{-2}, well width $w=80$ Å, impurity spread $d=2$ Å, and space layer $L_s=40$ Å for the case of the barrier-doped sample. It is apparent from Fig. 1 that moving the δ sheet from the center of the well to either the interface or into the barrier can lead to a significant change in the shape of the potential. The electron ground state, referenced to the lowest point in the corresponding conduction band, goes up drastically from 63 meV for the case of the center-doped layer to 115 meV for interface doping and to 169 meV for the barrier-doped structure. But the energy difference between the electron ground state ($E1$) to heavy-hole ground state (hh1) decreases only slightly from 1.282 to 1.260 and to 1.258 eV in the respective cases. In each sample the electron density at this doping level (2×10^{12} cm^{-2}) is about 1.7×10^{12} cm^{-2}, and only the subband $E1$ is occupied. So all the structures have achieved single-subband occupation at this doping level. The advantage of one-subband occupation is a better confinement of the electron distribution, which is useful for some device applications.

Figure 2 plots the change of the electron ground-state position and the energy difference between $E1$ and hh1 as a function of impurity distribution. The transition energy (between $E1$ to hh1) hardly changes with impurity broadening between 2–50 Å despite some reduction for $E1$. The change of $E1$ has been compensated by an opposite change of hh1. This is also found to be true when the doping density fluctuates within a certain range (e.g., ±20%). The transition energies change by less than 2 meV when the doping density varies from 1.8 to 2.2×10^{12} cm^{-2}. This behavior gives us an added confidence when comparing with experimental data, since the impurity spread and the doping density should be controlled within the respective ranges.

The effect of the surface states, which pin the Fermi level to the middle of the band gap, is to build an internal field by means of charge transfer. The amount of charge transferred to the surface states is dependent upon the thickness of the capping layer. When the thickness is increased from 50 to 500 Å, the charge transferred to the surface states is reduced from 4.7×10^{11} to 7×10^{10} cm^{-2} (Fig. 3).

As the doping density increases, the potential-energy diagram changes accordingly. For the case of the center δ-doped system, the second subband starts to populate at the doping density of 4.6×10^{12} cm^{-2} at zero temperature. The greatest single-subband 2DEG density is about 4.3×10^{12} cm^{-2} for this well width (80 Å). This greatest single-subband areal density decreases to 3.8×10^{12} cm^{-2} for the case of the interface-doped system and to just 2.2×10^{12} cm^{-2} for the δ-modulation-doped layer. The main limitation to the highest areal density for the barrier δ-doped system is a deepened V-shaped potential in

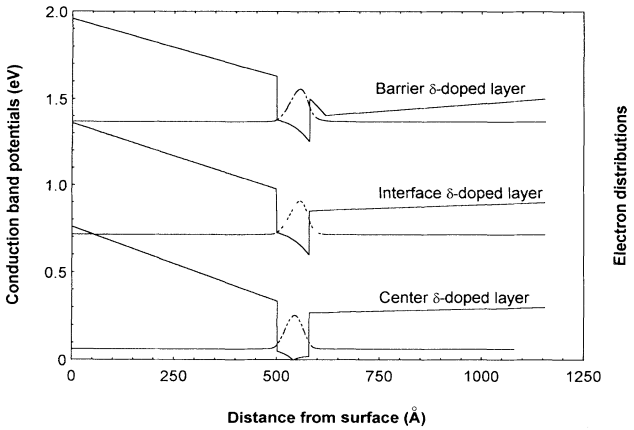

FIG. 1. The conduction-band potential profiles (solid lines) and electronic distributions (dashed lines) for the center, edge, and barrier δ-doped $In_xGa_{1-x}As$/GaAs quantum wells. The surface is on the far-left side at the zero point. The potentials for both the edge- and barrier-doped systems have been shifted vertically in order to assist the comparison.

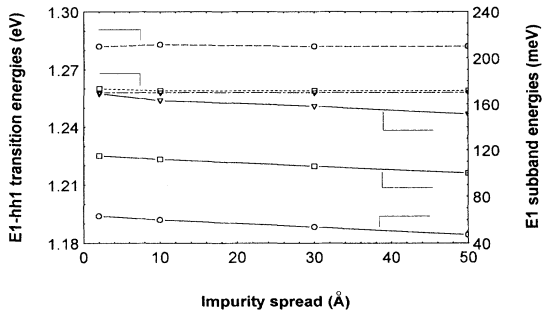

FIG. 2. The dashed or dashed-dotted lines are the transition energies (left Y axis) between $E1$-hh1 for the three selectively δ-doped systems. They barely change as the impurity spread increases from 2 to 50 Å. The solid lines are the $E1$ subband energies (right Y axis), respectively. They show a steady decrease as the impurity spread increases (open circle for the center δ-doped layer, open square for the bottom edge-doped layer, and open triangle for the barrier-doped case).

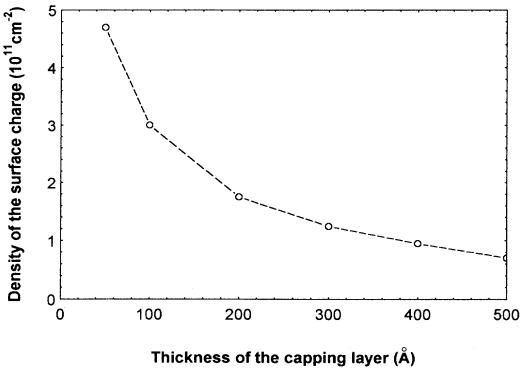

FIG. 3. Density of the charge transferred to the surface due to pinning as a function of the capping-layer thickness.

the barrier region as the δ-doping density increases. This V-shaped potential can lead to an extra confinement, which attracts electrons to the barrier. In fact, the lowest subband resides inside the V-shaped potential in the barrier when the doping level is above 4×10^{12} cm^{-2}, leaving very limited electron density inside the well. Figure 4 shows the potential diagram and the electronic distribution for this situation. Obviously, the mobility will drop now as the impurity scattering becomes strong. Further, the optical-oscillator strength will decrease because electrons become spatially separated from the photoexcited holes. So, theoretically, we find that there should be an optimal doping level for the δ-modulated-doped system. The highest single-subband occupation density decreases as the δ sheet moves away from the center, to the edge, and finally into the barrier.

III. EXPERIMENTAL DATA

All the samples studied here were grown using a VG Semicon V80 MBE system that has been described elsewhere.[18] The GaAs and $In_xGa_{1-x}As$ growth rates employed were approximately 0.75 and 1.0 μm/h, respectively, with an As_4 flux of $\sim10^{-5}$ mb. Buffer layers of at least 1 μm of GaAs were grown before the δ-doping/quantum-well region. A growth temperature of 450±10 °C was used for the active region, this being a compromise between inhibiting In and Si segregation and diffusion (low T) and obtaining good luminescence properties (high T). The active region consists of an 80-Å-thick $In_xGa_{1-x}As$ well plus a 500-Å GaAs capping layer, with a δ sheet placed at different positions as a complete set. The two-dimensional (2D) doping density is 2×10^{12} cm^{-2}. For the barrier δ-doped sample the space layer is 40 Å. The In concentration x is measured by photoluminescence to be 0.265 from an undoped reference sample grown under the same conditions.

Van der Pauw–Hall measurements were made for all samples and the mobilities at 77 K were found to be 1660 cm^2/V s for the center-doped sample (Al2023), 2172 cm^2/V s for the edge-doped one (Al2026), and 3642 cm^2/V s for the barrier-doped layer. The photoluminescence (PL) measurements were taken with the samples cooled in a continuous-flow variable-temperature He cryostat. The 633-nm line from a He-Ne laser was used as the excitation source. The excitation intensity was low (<0.1 W/cm^2), so the perturbation to the majority-carrier population was negligible. Figure 5 shows their low-temperature (2.5 K) PL spectra. The PL data from the reference sample (Al204) is also included for comparison. A notable feature of these spectra is the redshift (about 20 meV) in the peak position as the δ sheet moved from the center (sample Al2023) to the edge (Al2026). The shift is much smaller (2 meV) between the interface-(Al2026) and the barrier-(Al2025) doped layers. This behavior is in very good agreement with our self-consistent calculation results, which predicted a large shift (22 meV) between samples Al2023 and Al2025, and a small shift (2 meV) between Al2026 and Al2025. Another feature in the spectra is the decrease of the relative PL intensity and narrowing of the signal width. One may argue that these are due to the difference of the overlap between electron and hole wave functions, but our separate calculation shows that they all have good overlap for this narrow well width (80 Å) and doping density. We think that these effects may result from a different

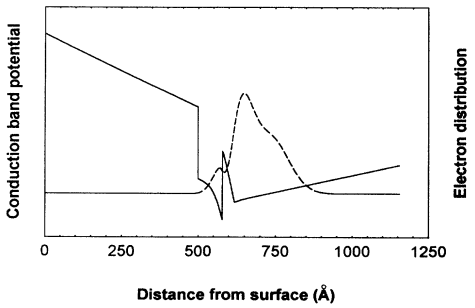

FIG. 4. Potential diagram (solid line) and electronic distribution (dashed line) for the barrier δ-doped system at a doping level of 4×10^{12} cm^{-2}.

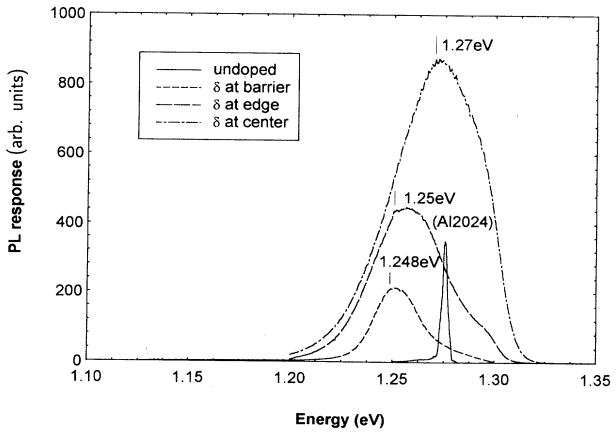

FIG. 5. Photoluminescence spectra at 2.5 K for the three selectively δ-doped samples. The PL data for the undoped reference sample is also shown. The peak positions were identified by a numerical fitting procedure.

hole-localization mechanism. More work is under way to resolve this issue.

Although the self-consistent calculations correctly predict the variation in the transition energies from one sample to the next, the actual transition energies are not given particularly accurately for any one of the samples. Transition energies of 1.282, 1.260, and 1.258 eV are predicted for Al2023, Al2026, and Al2025, respectively, but the experimental values are 1.270, 1.250, and 1.248 eV. The experimental values are, therefore, about 10 meV smaller than those predicted by the calculation. This energy discrepancy is unlikely to have resulted from interfacial broadening since our undoped reference sample, grown under identical conditions, gives a rather narrow spectrum (Fig. 5). Further, although one may argue that a small change in well width may account for the discrepancy, our detailed calculation reveals that the well would have to be widened by 10 Å in order to explain the experimental data. This appears unlikely for two reasons. First, MBE can control the well width much better than 10 Å, variation by 1 ML (2.8 Å) is conceivable, but not 10 Å. Second, the PL data from the reference sample, grown under identical conditions, are consistent with an 80-Å well width, so we find it implausible that the doped samples should have 90-Å well. In other words, the energy is not sensitive enough to the well width when the well is 80 Å wide or above. Instead, we think that this energy-gap narrowing may be due to many-body effects that have been reported widely before.[19] Many theories have been proposed to calculate the effect, but most have so far overestimated the renormalization. We study them in the next section.

IV. BAND-STRUCTURE RENORMALIZATION

As is well known, the Coulomb interaction between carriers can lead to reduction of the band gap via the many-body effects of exchange and correlation. These effects cannot be adequately accounted for by the use of single-particle equations, such as those of Kohn and Sham.

Many attempts to quantify the band-gap renormalization have appeared in the literature. A simple one is the empirical formula $\Delta E = -3.1(na_0^2)^{1/3}E_0$ used by Schmitt-Rink and Ell,[19] which leads to a 50-meV energy reduction for our structure. (E_0 is the 2D excitonic Rydberg, and a_0 the corresponding Bohr radius.) The static plasmon-pole approximation (PPA), which has been used by us and various other groups before,[20,21] results in self-energies of 17 meV due to screened exchange and 13 meV due to the Coulomb hole for the $n=1$ electron subband. The heavy-hole $n=1$ subband (hh1) has an identical Coulomb hole contribution of 13 meV in our static approximation, giving a total renormalization of 43 meV (a reduction) for the transition between $E1$ and hh1. These results overestimate the renormalization considerably since only 10–12 meV has been observed in our experimental data. As the discrepancy is greater than the uncertainty in either the experiments or the self-consistent calculations, we believe we must refine our estimate of the self-energy.

Note that static PPA calculations are occasionally described as random-phase approximation (RPA) (e.g., abstract of Ref. 22), but that the results from PPA can be significantly different from RPA in quasi-2D systems.[23] For this reason we have also used the fully dynamical RPA to estimate the band-gap renormalization for our center-doped structure.

Within RPA the dielectric properties of the electron gas are approximated by the linear response of a gas of independent carriers. This incorporates the effects of screening and plasma oscillations due to the long range of the Coulomb potential. The RPA dielectric function is then used to estimate the screened interaction between carriers, and the resulting correction to the energy of a single particle (the self-energy) is evaluated in first-order perturbation theory (the so-called GW approximation). Each calculated self-energy then requires a twofold integration over the wave vector and imaginary frequency,[24] instead of a single integration over the wave vector, so that the computational effort is considerably greater than in PPA.

Contributions of the second and higher orders (vertex corrections) are neglected: when they are included consistently within the Hubbard approximation[24,25] their effect is very small at the high densities considered here.

A more hazardous approximation has been made in treating the polaronic renormalization of the bands. For simplicity we use the zero-frequency dielectric constants throughout RPA calculations on the quasi-2D coupled electron-phonon system[23,26] suggest that at the densities of interest our results could be in error by up to 5% of the total renormalization.

Single-particle wave functions enter the RPA calculation via matrix elements of the Coulomb potential, which we have calculated using the Hartree wave functions of the states $E1$, $E2$, hh1, and hh2. In addition to truncating with respect to the subband index, we use a parabolic in-plane dispersion for the electrons and heavy holes. One effect of strain is to lighten the hh mass in the plane; we have taken $m\text{hh}=0.1$, but the final result for the correlation energy of the hole is insensitive to the precise value, varying by only 0.6 meV when $m$hh varies between 0.07 and 0.15.

With these approximations we find a total band-gap reduction of 25 meV at $k=0$, the center of the Brillouin zone, which is tolerably close to the observed result. Only 0.4 meV of this is due to virtual transitions to the unoccupied states $n=2$, so that it would be an excellent approximation to ignore the higher subbands. Note that a strictly 2D calculation gives a significantly higher result, 39 meV.

V. CONCLUSION

We have made a theoretical and experimental study of some selectively δ-doped strained $In_xGa_{1-x}As/GaAs$ quantum wells. Our self-consistent calculation reveals changes to the potential profile as the δ sheet is moved away from the center towards the edge and into the barrier. The calculation also reveals an optimal value for the density in the barrier-doped system, beyond which the electrons will be attracted into the doping region. Exper-

imentally, we present evidence that the edge δ-doped layer can have both good optical and electrical properties despite the possible existence of the interface states. The electron mobility increases as the δ sheet is moved away from the center to the edge, and increases further when it is moved into the barrier. Good agreement has been obtained between PL data and the calculated results. Many-body renormalization effects have been included through both static plasmon-pole and fully dynamical random-phase approximations. The RPA calculation turns out to be much closer to the experimental observations than the others.

ACKNOWLEDGMENTS

The authors have benefited from discussions with C. Matthai, P. Dawson, and M. Elliot. We would also like to acknowledge the financial support from EPSRC.

[1]A. Zrenner, F. Koch, R. L. Williams, R. A. Stradling, K. Ploog, and G. Weimann, Semicond. Sci. Technol. **3**, 1203 (1988).

[2]E. F. Schubert, T. H. Chiu, J. E. Cunningham, B. Telland, and J. B. Stark, J. Electron. Mater. **17**, 527 (1988).

[3]Mao-long Ke, J. S. Rimmer, B. Hamilton, J. H. Evan, M. Missious, K. E. Singer, and P. Zalm, Phys. Rev. B **45**, 14 114 (1992).

[4]M. H. Degani, Phys. Rev. B **44**, 5580 (1991).

[5]T. H. Shen, M. Elliot, A. E. Fowell, A. Cafolla, B. E. Richardson, D. Westwood, and R. H. Williams, J. Vac. Sci. Technol. B **9**, 2219 (1991).

[6]F. Capasso, A. Y. Cho, K. Mohammed, and P. W. Foy, Appl. Phys. Lett. **46**, 664 (1985).

[7]Mao-long Ke and B. Hamilton, Phys. Rev. B **47**, 4790 (1993).

[8]W. T. Masselink, Phys. Rev. Lett. **66**, 1513 (1991); Appl. Phys. Lett. **59**, 694 (1991).

[9]J. Wagner, A. Fischer, and K. Ploog, Phys. Rev. B **42**, 7280 (1990).

[10]C. I. Harris, H. Kalt, B. Monemar, and K. Kohler, Surf. Sci. **263**, 462 (1992).

[11]J. J. Harris, R. Murray, and C. T. Foxon, Semicond. Sci. Technol. **8**, 31 (1993).

[12]J. E. Cunningham, W. T. Tsang, G. Timp, E. F. Schubert, A. M. Chang, and K. Owusu-Sekyere, Phys. Rev. B **37**, 4317 (1988); T. Y. Kuo, J. E. Cummingham, E. F. Shubert, W. T. Tsang, T. H. Chiu, F. Ren, and C. G. Fonstad, J. Appl. Phys. **64**, 3324 (1988).

[13]L. Chico, W. Jaskolski, R. Perez-Alvarez, and F. Garcia-Moliner, J. Phys. Condens. Matter **5**, 9069 (1993).

[14]G. T. D. Huang, U. K. Reddy, T. S. Henderson, R. Houdre, and H. Morkoc, J. Appl. Phys. **62**, 3366 (1987).

[15]U. K. Reddy, G. J. T. Henderson, D. Huang, R. Houdre, H. Morkoc, and C. W. Litton, J. Vac. Sci. Technol. B **7**, 1106 (1989).

[16]Sadao Adachi, J. Appl. Phys. **53**, 8775 (1982).

[17]J. Y. Marzin, M. N. Charasse, and B. Sermage, Phys. Rev. B **31**, 8298 (1985).

[18]D. I. Westwood, D. A. Woolf, and R. H. Williams, J. Cryst. Growth **98**, 782 (1989).

[19]G. E. W. Bauer and T. Ando, Phys. Rev. B **31**, 8321 (1985); V. D. Kulakovskii, E. Lach, A. Forchel, and D. Grutzmacher, *ibid.* **40**, 8087 (1989); S. Schmitt-Rink and C. Ell, J. Lumin. **30**, 585 (1985).

[20]Mao-long Ke, M. Godfrey, P. Dawson, and B. Hamilton, Appl. Phys. Lett. (to be published).

[21]G. Livescu, D. A. B. Miller, D. S. Chemla, M. Ramaswamy, T. Y. Chang, N. Sauer, A. C. Gossard, and J. H. English, IEEE J. Quantum Electron. **24**, 1677 (1988).

[22]C. Ell and H. Haug, Phys. Status Solidi B **159**, 117 (1990).

[23]S. Das Sarma, R. Jalabert, and S.-R. E. Yang, Phys. Rev. B **41**, 8288 (1990).

[24]G. D. Mahan, *Many-Particle Physics* (Plenum, New York, 1981).

[25]J. Hubbard, Proc. R. Soc. London Ser. A **240**, 539 (1953); T. M. Rice, Ann. Phys. (N.Y.) **31**, 100 (1965); C. S. Ting, T. K. Lee, and J. J. Quinn, Phys. Rev. Lett. **34**, 870 (1975); I. K. Marmorkos and S. Das Sarma, Phys. Rev. B **44**, 3451 (1991).

[26]R. Jalabert and S. Das Sarma, Phys. Rev. B **40**, 9723 (1989).